# Zero offset VSP processing for coal reflections

Salman K. Bubshait and Don C. Lawton

## ABSTRACT

Shlumberger has acquired five VSP surveys on behalf of EnCana in Alberta. The primary goal of the VSP surveys is to study the azimuthal variations in the AVO response of the coals of the Mannville Formation. The zero-offset VSP survey was processed using VISTA through to corridor stack, and shows high reflection quality

## INTRODUCTION

Vertical Seismic Profiling (VSP) is used to obtain several rock properties as well as to acquire a seismic image of the subsurface that helps with surface seismic interpretation and processing. Rock properties obtained from VSP surveys include velocity, attenuation, impedance and anisotropy. In addition, VSP surveys are used in the analysis of wave propagation (Stewart, 2001).

There are several ways in which a VSP survey is conducted. If a source is located tens of meters away from the borehole containing the receivers, then it is a "Zero Offset VSP Survey." Also, if the source is shot at several offsets from the borehole, then it is called a "Walk-away VSP Survey" or "Multi-Offset VSP Survey." In addition, if sources are at several azimuths from the borehole, the survey is called "Multi-Azimuth Survey." All of the surveys mentioned so far provide 2D images of the subsurface. A 3D image also can be obtained with a full areal set of sources (Stewart, 2001).

The purpose of acquiring different VSP surveys depends on the goal of the survey. A zero-offset VSP survey can provide information about the time-depth conversion, normal incidence reflectivity and interval velocities in depth. On the other hand, a multi-offset VSP survey could be used for AVO analysis. Generally, the VSP surveys mentioned above have receivers down the borehole and the sources on the surface (Stewart, 2001).

## GEOLOGICAL BACKGROUND

One of the purposes of the VSP acquisition is to examine the Lower Cretaceous Mannville coal fracture systems. These fractures, better known as face and butt cleat fracture systems, are permeability conduits for methane production. In general, the amount of methane gas within porous coal systems is larger than that of conventional gas around the world. However, most of the coal bed methane (CBM) systems have not been produced. Figure 1 shows a stratigraphic sequence of coal bearing formations in Alberta. Figure 2 shows the dominant stress direction in the Western Canadian Sedimentary Basin.
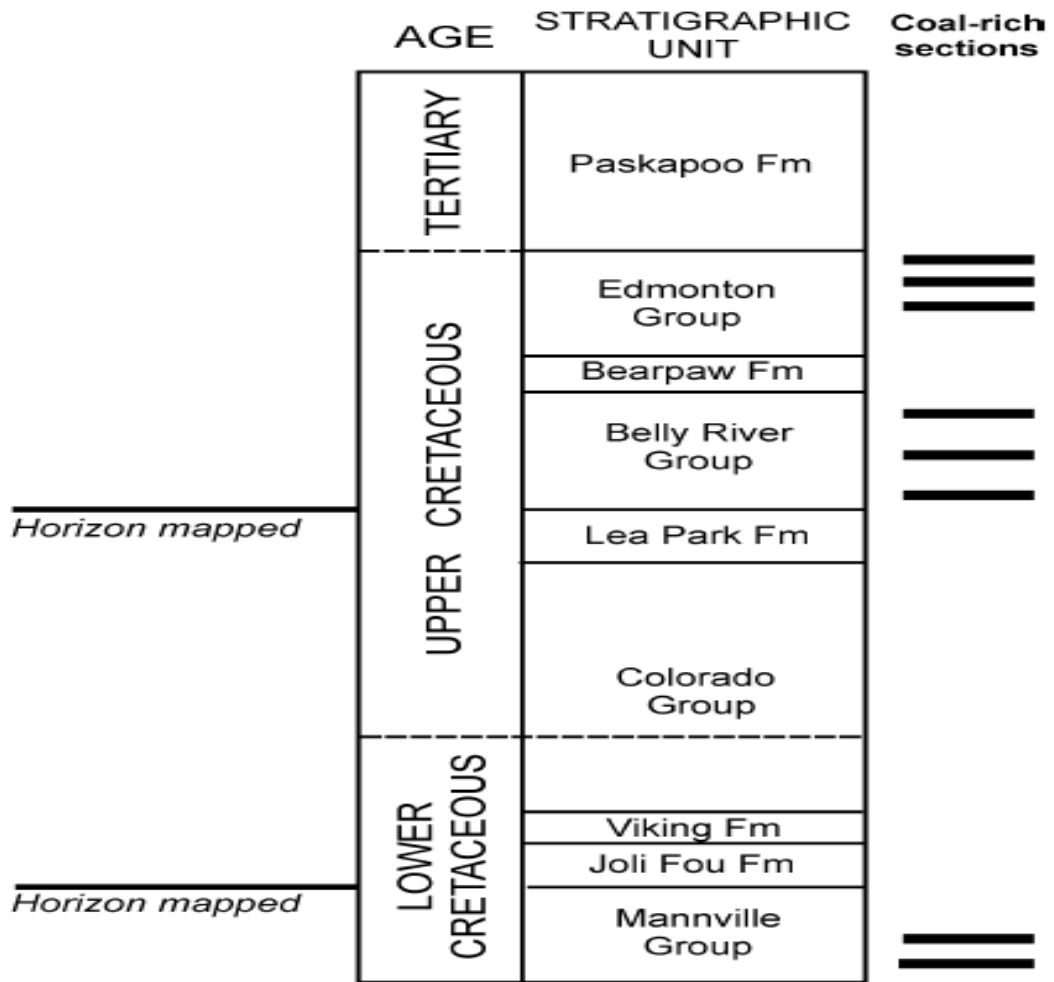
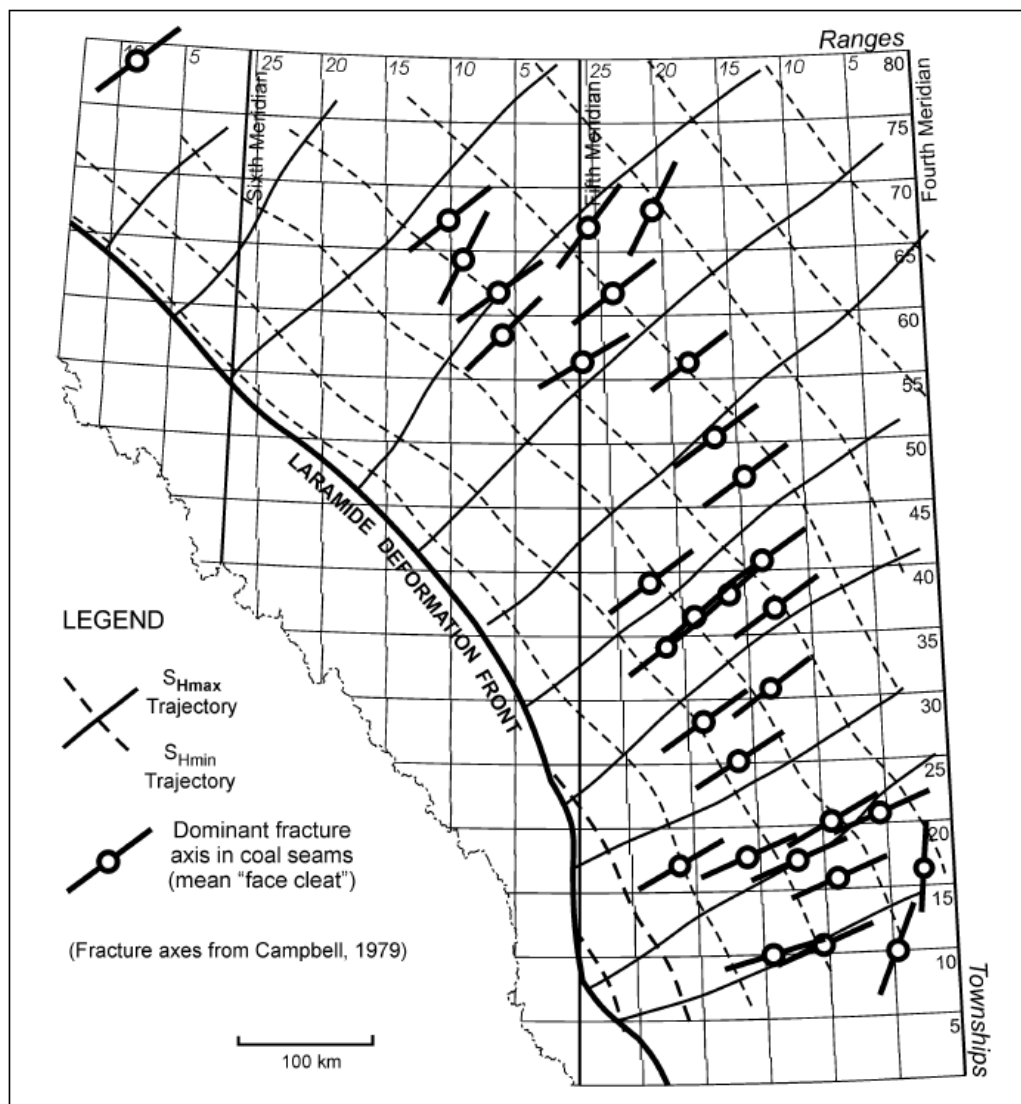FIG. 1. Stratigraphic geological sequence of coal bearing formations in Alberta (Bell and Bachu, 2003).

FIG. 2. The maximum stress direction is NE-SW which is parallel to the face cleats (Bell and Bachu).

## THEORY OF ZERO OFFSET VSP PROCESSING FLOW

VSP surveys have advantages over surface seismic surveys in terms of data. One advantage is the ability to separate the downgoing (direct) and upgoing (reflected) wavefields that enable the calculation of true reflection amplitude or seismic impedance. The results of the calculation permit the correlation between well logs and surface seismic on one hand with the VSP result in the other. Of course, VSP data have enhanced high frequency content because waves travel through the low velocity level only once. This may help in the detection of reflectors not seen on the surface seismic data. Also, the generation of corridor stacks can help eliminated inter-bedded multiples on both VSP and surface seismic data (Parker and Jones, 2008).

In VSP processing, the first step is to set up the geometry of zero-offset VSP. That enables the processor to pick first breaks which are used to flatten the data for upgoing

and downgoing separation, to invert for interval velocities, for time depth conversion, and for flattening of events by doubling the first break times (Coulombe, 1993).

The next step of VSP processing is wavefield separation. There are several methods of wavefield separation including: median filtering, F-K filtering, K-L transform, tau-p transform (Hinds et al., 1999). Median filtering enhances the downgoing waves which are then subtracted from the raw data to give the upgoing waves (Coulombe, 1993).

The downgoing waves are then flattened using first break times, trace equalized to account for spherical spreading and transition losses and to avoid introducing trace-by-trace effects to the data, then a deconvolution operator is designed. The deconvolution operator is applied to the upgoing waves and the waves are scaled by the same factor used on the upgoing waves. Reflection coefficients are then calculated from the ratio of upgoing to downgoing wave. After deconvolution, propagation effects such as some multiples are eliminated (Coulombe, 1993).

The last processing step is to shift the upgoing waves by the first break times to get two way time. Also, data are NMO corrected in the process. A corridor is used to account for propagation effects of upgoing waves, such as inter-bed multiples, and include reflections from below the well (Coulombe, 1993).

## PROCESSING OF ZERO OFFSET VSP DATA

The dataset processed in this section was acquired by Shlumberger on behalf of EnCana Corporation in Alberta. The well used has a zero-offset VSP, Three azimuth walkaway VSPs and a sparse 3D walkaway VSP survey was acquired. This report is concerned with processing of the zero-offset VSP data set. The primary objective of the surveys is to study the azimuthal properties in the AVO response of the Mannville coals. Figure 3 shows a map of the surveys acquired (Parker and Jones, 2008).
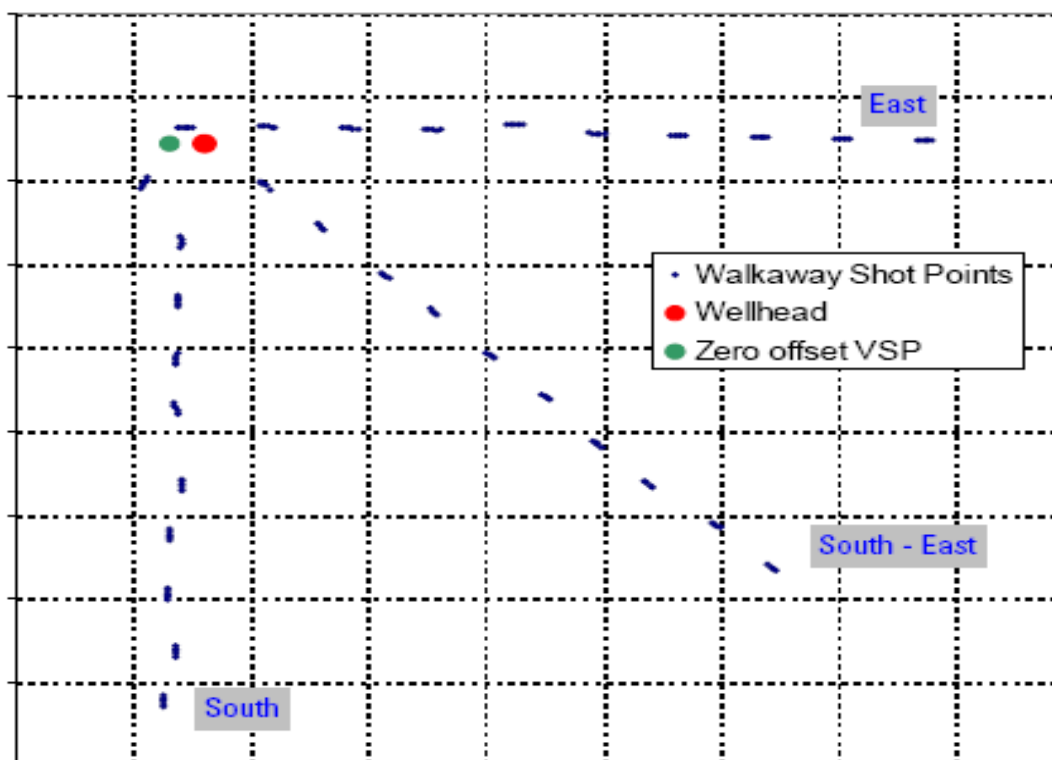
FIG. 3. Map of the VSP surveys acquired in Alberta. Maximum offset is 1500 m.

The zero-offset VSP was acquired by two Litton truck mounted vibroseis units with a 62 m offset and an azimuth of 269 degrees. A VSI tool with sixteen shuttles was used in the acquisition of the VSP data from depths 1420 – 48.7 m measured depth from Kelly bushing and 1 ms sampling rate. The receiver spacing is 15.1 m. A minimum of seven shots with sweep of 12 s consisting of frequency of 8-120 Hz were acquired with a 3 second design window. The vertical well had a Kelly bushing of 872.2 m above mean sea level (MSL) while the ground level is 868.1 m above MSL.

The zero-offset VSP was processed using VISTA, a processing program provided by GEDCO. After referring to the log report, the geometry of the zero-offset VSP has been set, with channel numbers 1, 2, 3, corresponding to X, Y and Z components are given Trace Code ID of 1, 3 and 2 for X, Y, Z respectively. Next, the velocity of the raw data are picked and displayed in Figure 4.
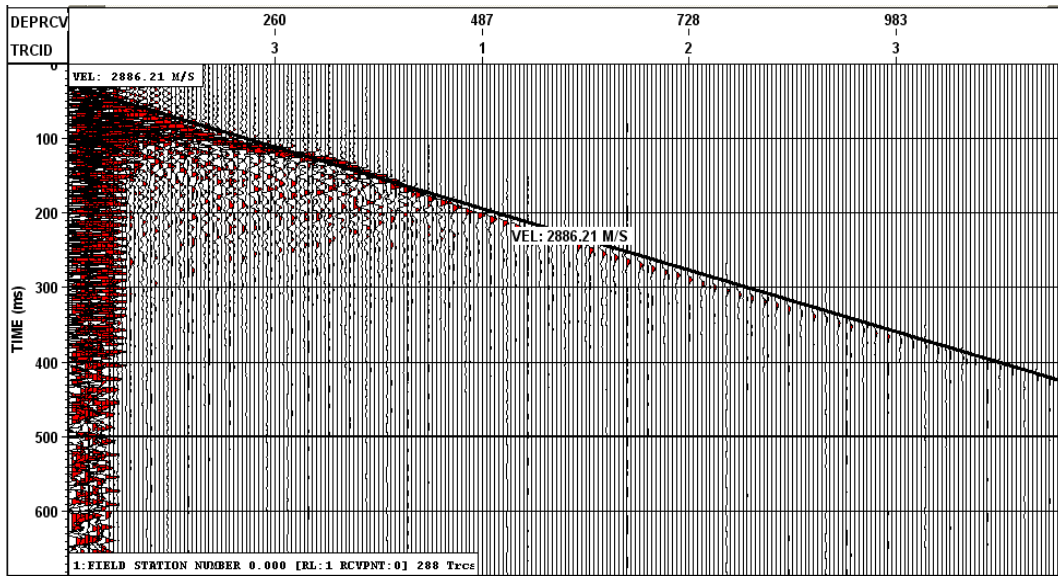
FIG. 4. Raw data with first break velocity of 2886.21 m/s displayed.

Now that the geometry and velocity of first breaks are set, the first breaks on each component of the data can be picked using the first trough of the first continuous event. Figures 5-8 show each raw component data with the first breaks picked and one where the Z component has AGC applied. Notice the dominance of downgoing waves in the vertical Z component.
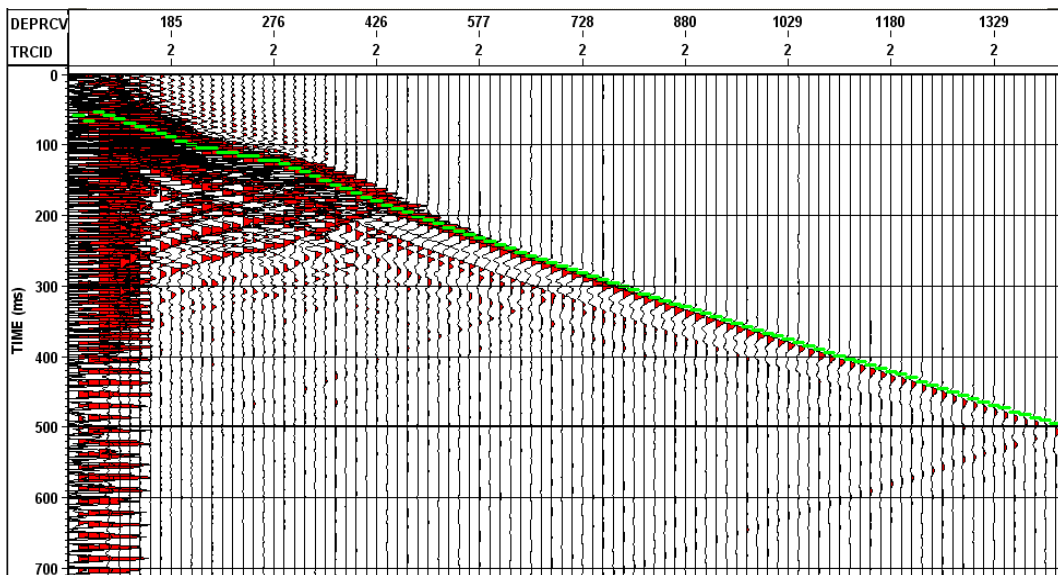


FIG. 5. Raw Z component with first break picked on the trough. Notice the dominance of the downgoing waves with comparison to the horizontal components.
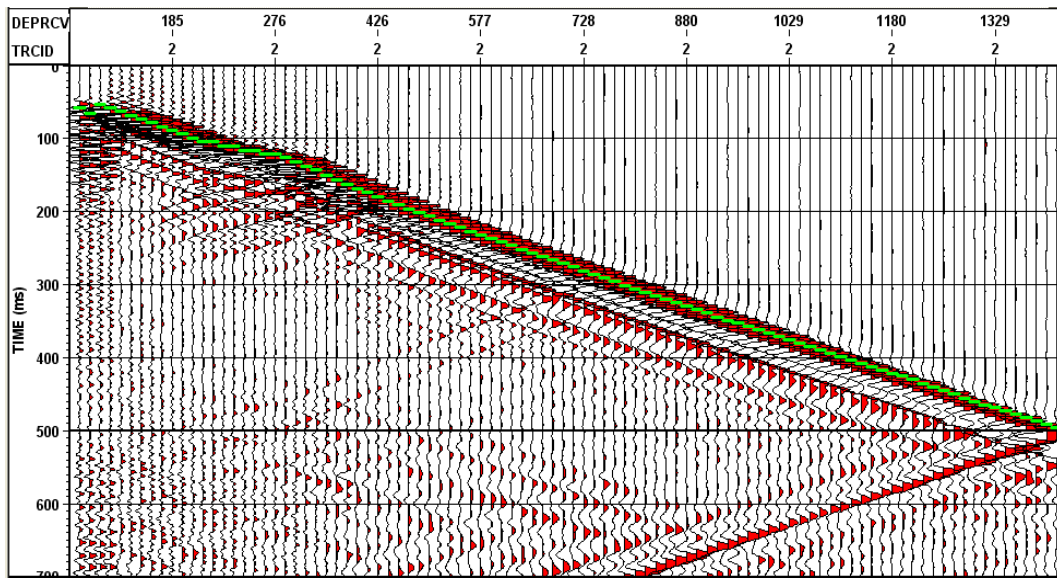
FIG. 6. Same raw Z component shown in Figure. 5. but with AGC applied.

.
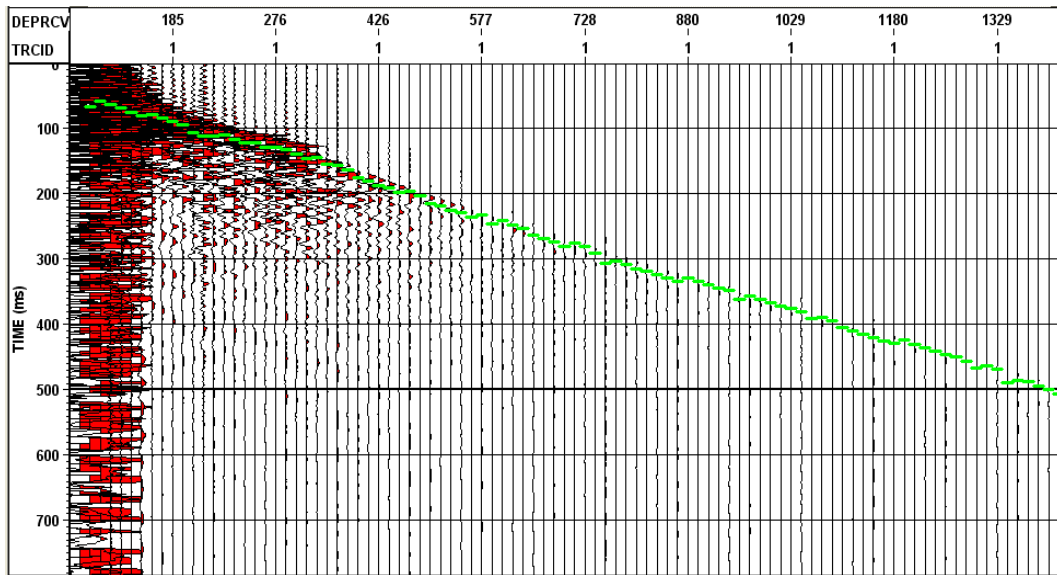
FIG. 7. Raw X component with first break picked on the trough.
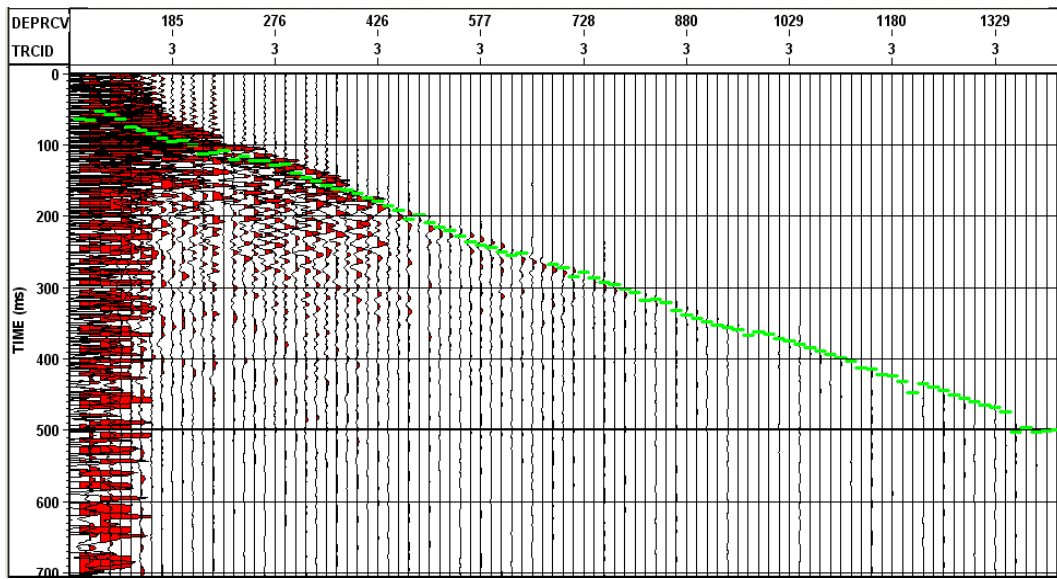
FIG. 8. Raw Y component with first break picked on the trough.

A QC plot of the first breaks as they are picked on each component is displayed in Figure 9. The figure shows that first break times increase when plotted with receiver depth. The three curves are color coded with Trace Code ID where 1, 2 and 3 represent the X, Z and Y component respectively. In this situation, the interest lies with the light blue color representing the Z component first breaks which is showing the most consistency.
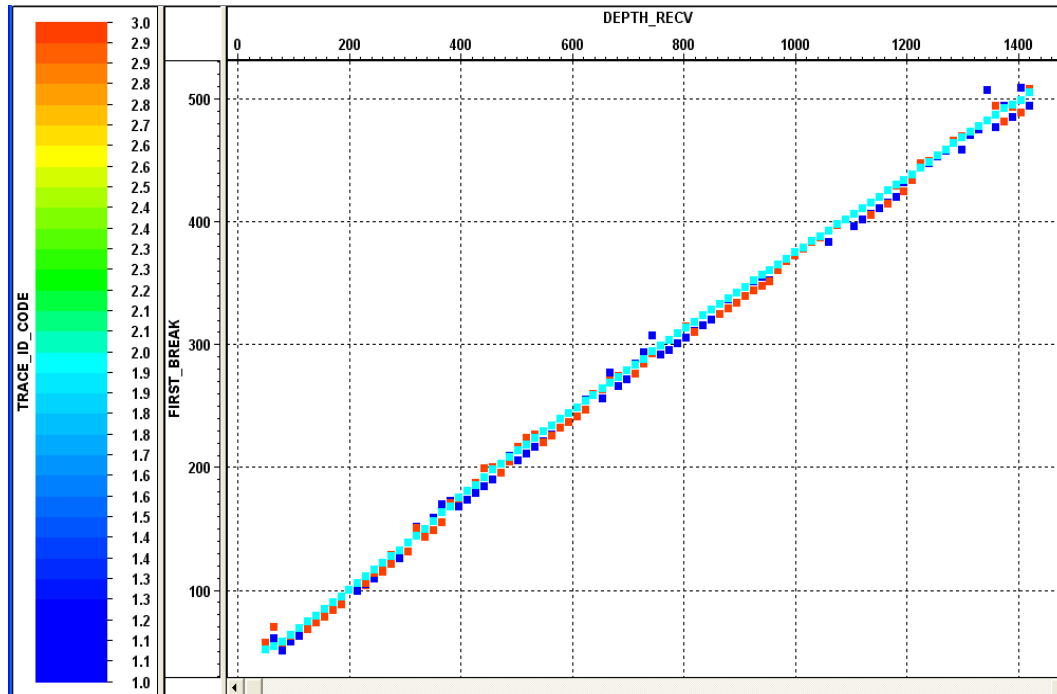


FIG. 9. QC plot of the first break times versus the depth of the receivers and color coded with Trace Code ID. The consistent light blue color is the one representing the vertical Z component first breaks that are of interest to us in the processing of zero-offset VSP.

Now that the first breaks are picked, the interval velocities based on the first breaks of the raw vertical Z component are calculated, stored and displayed in Figure 10.
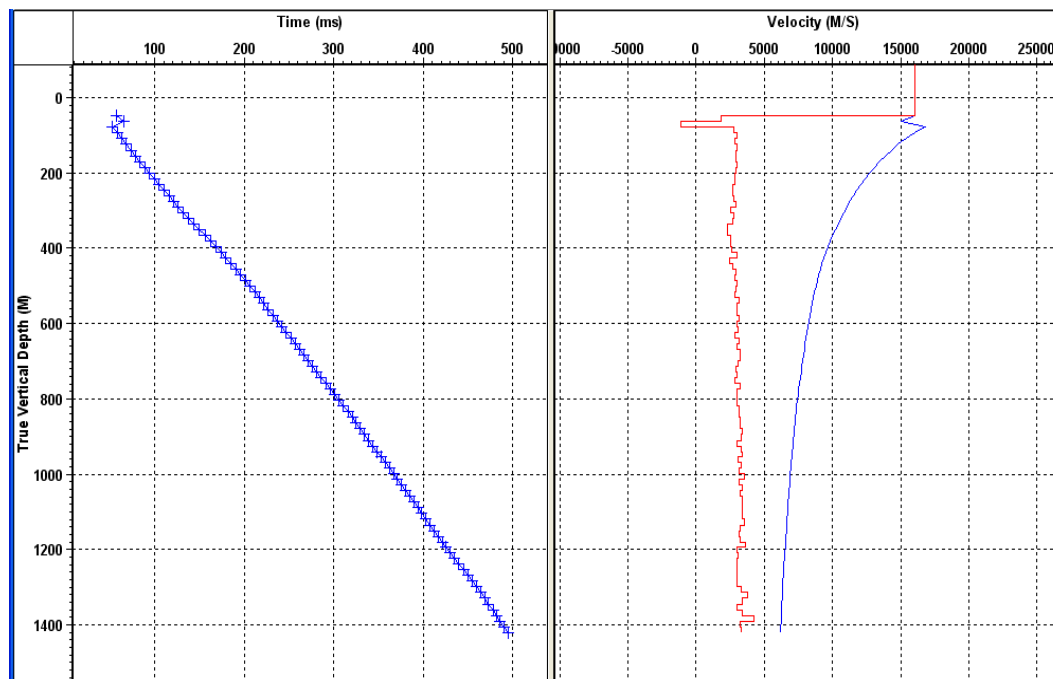


FIG. 10. The left shows the first break times of the raw vertical component plotted against depth. The right shows the corresponding interval velocities based on the figure to the left.

The next major processing step is to separate the downgoing from upgoing wavefields. Median filtering is the method that I chose to separate the wavefields and tested different lengths of median filtering, which consist of 9, 11, 13, 14, 15. Since there was no distinct difference in the median filtered upgoing waves, my analysis was mainly based on the isolation of the downgoing waves. In the end, I decided to go with 13 point median filtering since it best isolated the downgoing waves and showed the most continuous and coherent downgoing events and eliminated the upgoing waves best in the Z(-TT) section. The Z(-TT) section represents the vertical raw Z data flattened and bulk shifted to the datum. Figure 11 shows the flow used for wavefield separation.
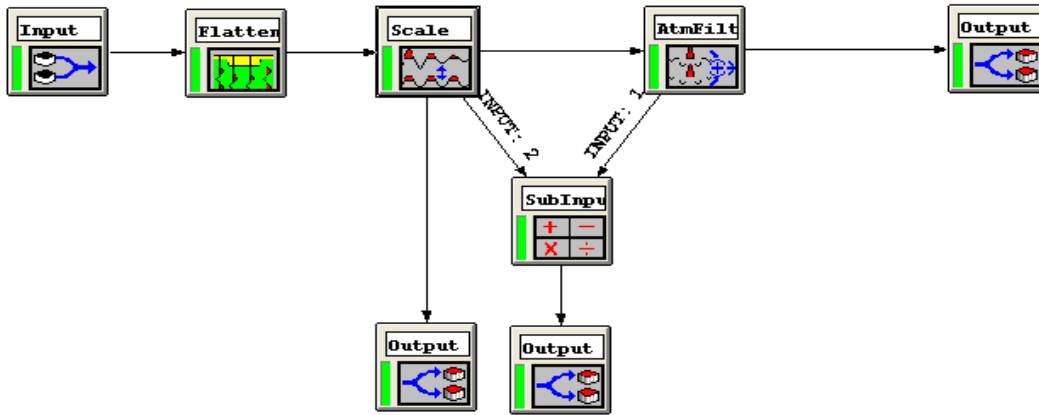
FIG. 11. The wavefield separation flow used to isolate the downgoing waves and then subtract them from the raw data to get the upgoing Z wavefield.

The above displayed flow deals with the raw Z vertical data as input sorted with Trace Code ID. The data is then flattened to the first break times and a mean filtering is performed to cover the direct arrivals only. That take us to our first output which is the Z(-TT) data representing the raw Z vertical data flattened to first breaks and bulk shifted to first break times. Median filtering is applied to the result and then subtracted from the original data. Then the median filtered upgoing and downgoing vertical Z(-TT) data are displayed. Figure 12 displays the flattened and mean scaled Z(-TT). Figures 13-15 show the downgoing median filtered data in which the decision to go with 13 point median filtering is based on. The corresponding 13 point median filtered upgoing Z(-TT)is displayed in Figure 16.
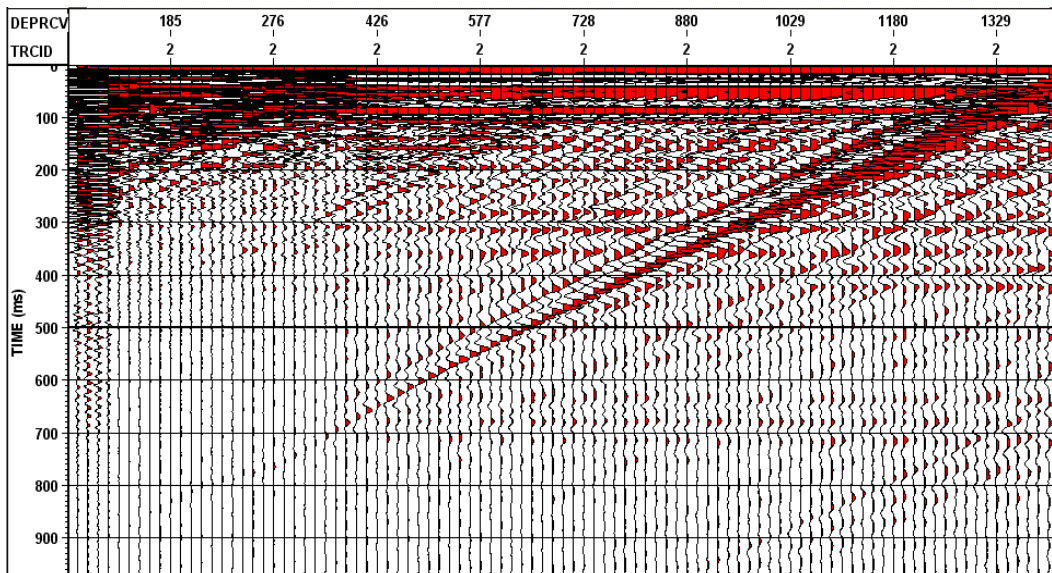


FIG. 12. Flattened and mean scaled Z(-TT) data.
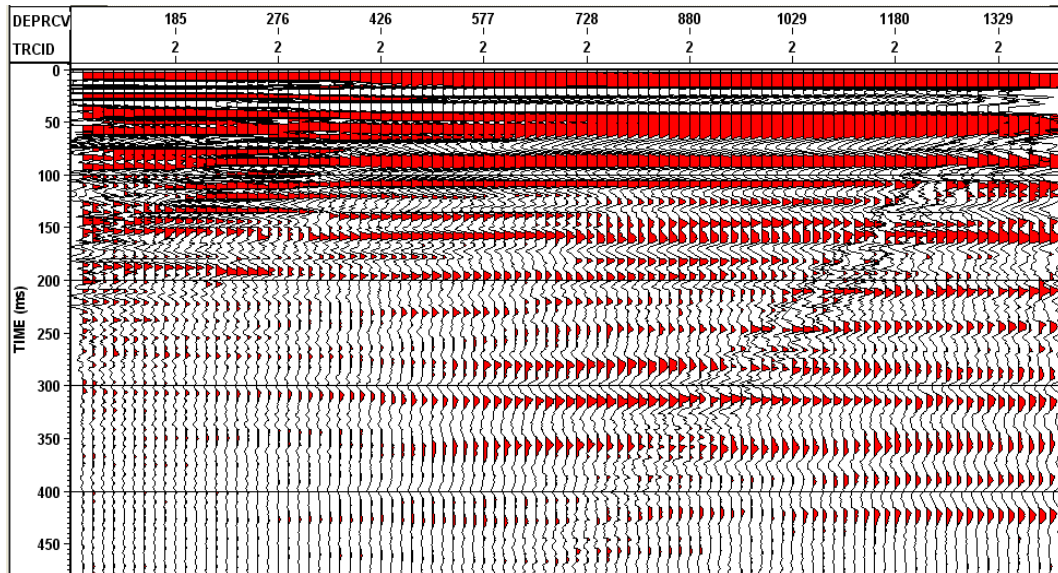
FIG. 13. Downgoing Z(-TT) with 11 point median filtering after subtracting upgoing waves.
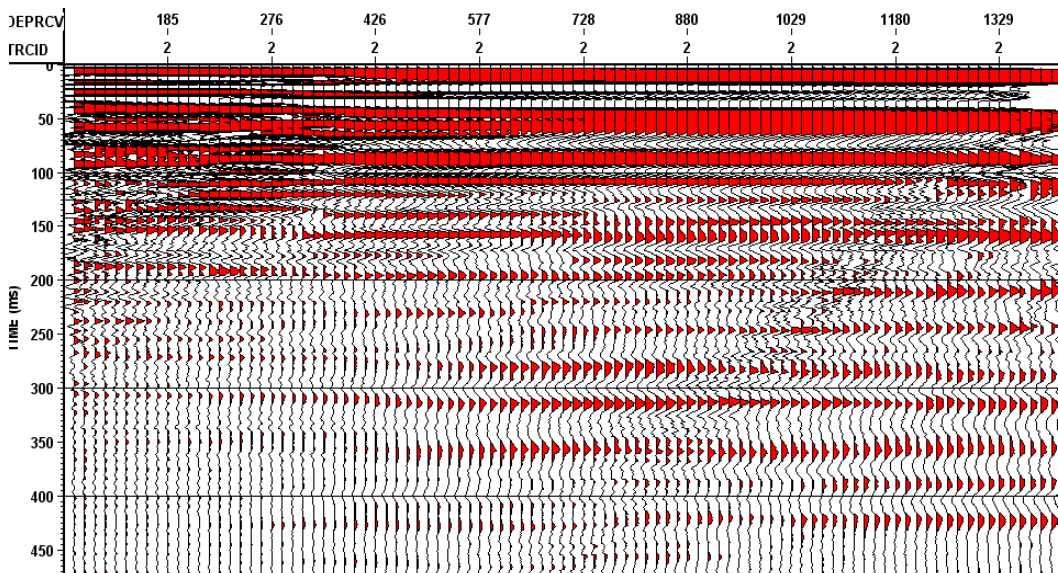


FIG. 14. Downgoing Z(-TT) with 13 point median filtering after subtracting upgoing waves. Notice that this filtering length produces the most continuous and coherent downgoing events while best eliminating the upgoing waves. This is the length that will be used in further processing steps.
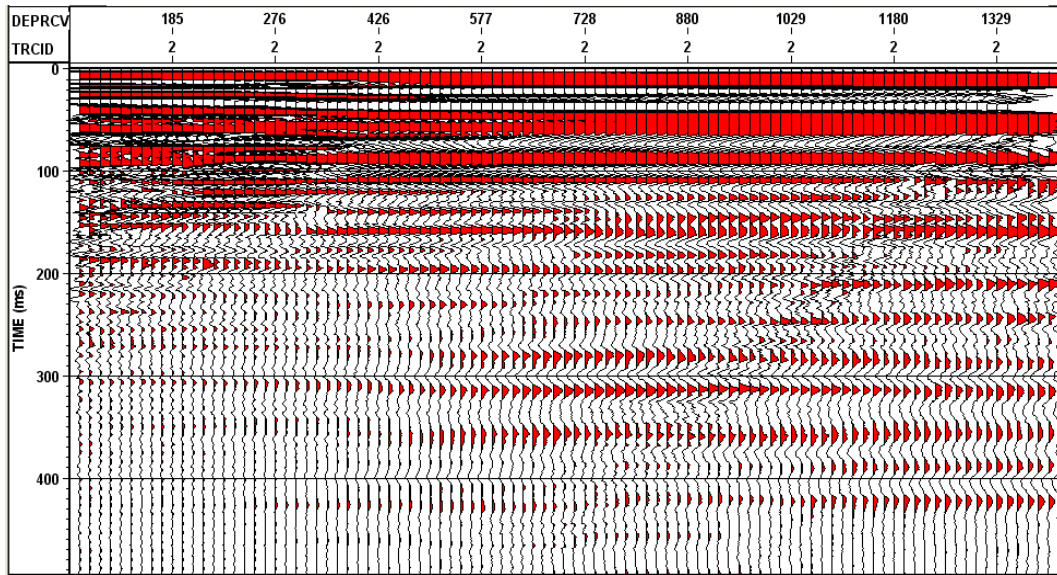
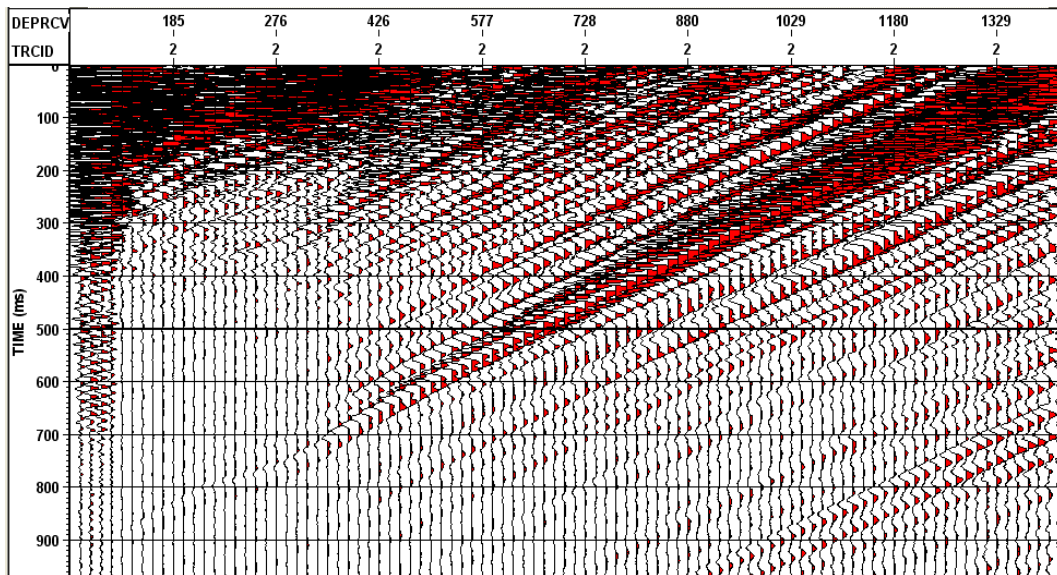FIG. 15. Downgoing Z(-TT) with 15 point median filtering after subtracting upgoing waves.



FIG. 16. Upgoing Z(-TT) with 13 point median filtering after subtracting downgoing waves. This is the result used in further processing steps.

Now that the upgoing and downgoing wavefields are separated, the upgoing wavefields can be displayed in Z(FRT) or "Field Record Time" and in Z(+TT) where +TT indicates two-way-time by multiplying the first breaks with two. Figure 17 shows upgoing Z(FRT) and Figure 18 shows upgoing Z(+TT). Figure 19 shows the same Z(+TT) in Figure 18 but with AGC applied.
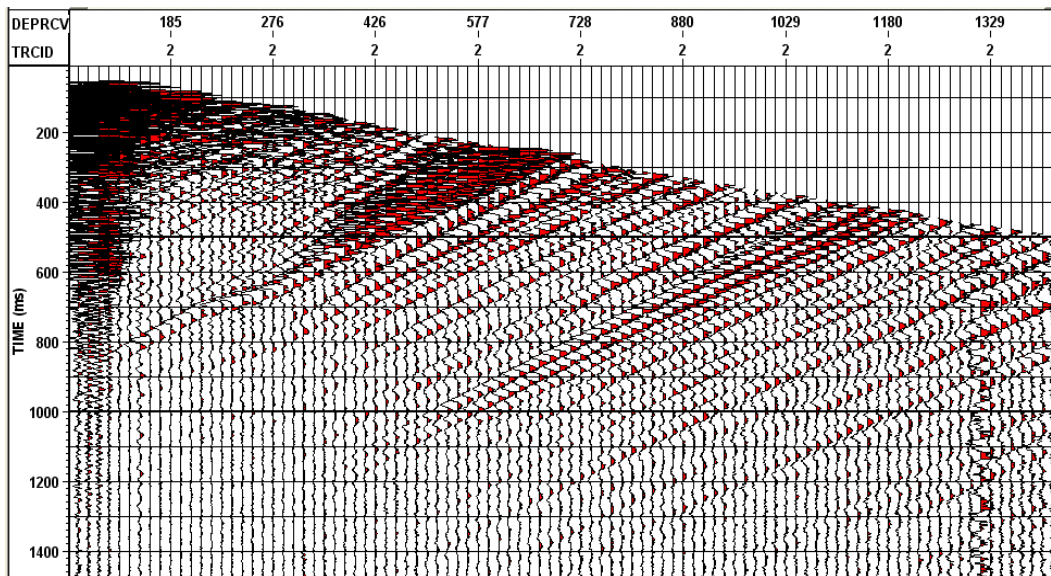
FIG. 17. Upgoing Z component in field record time Z(FRT).
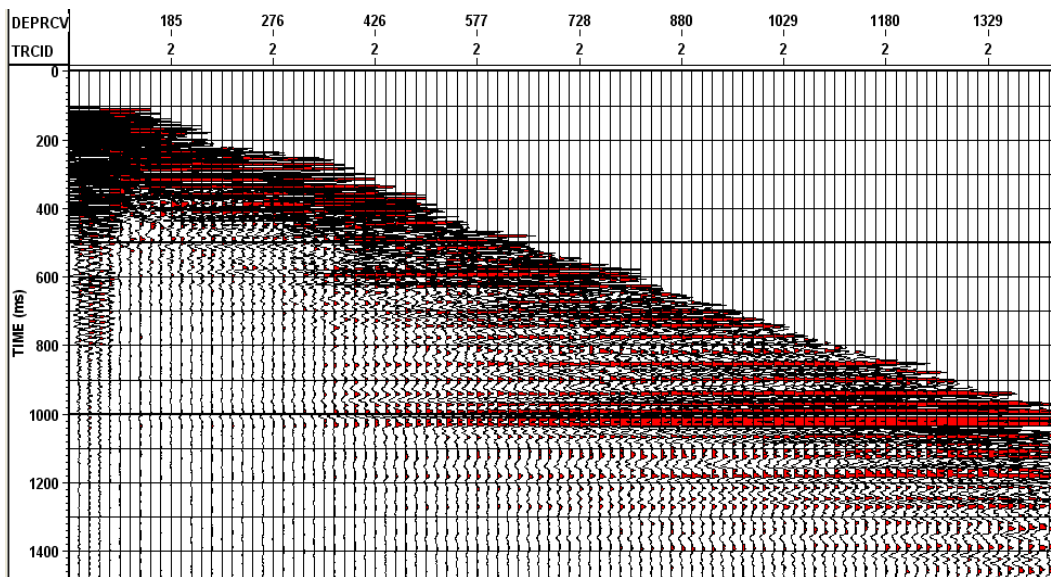


FIG. 18. Upgoing Z component in two-way-time Z(+TT).
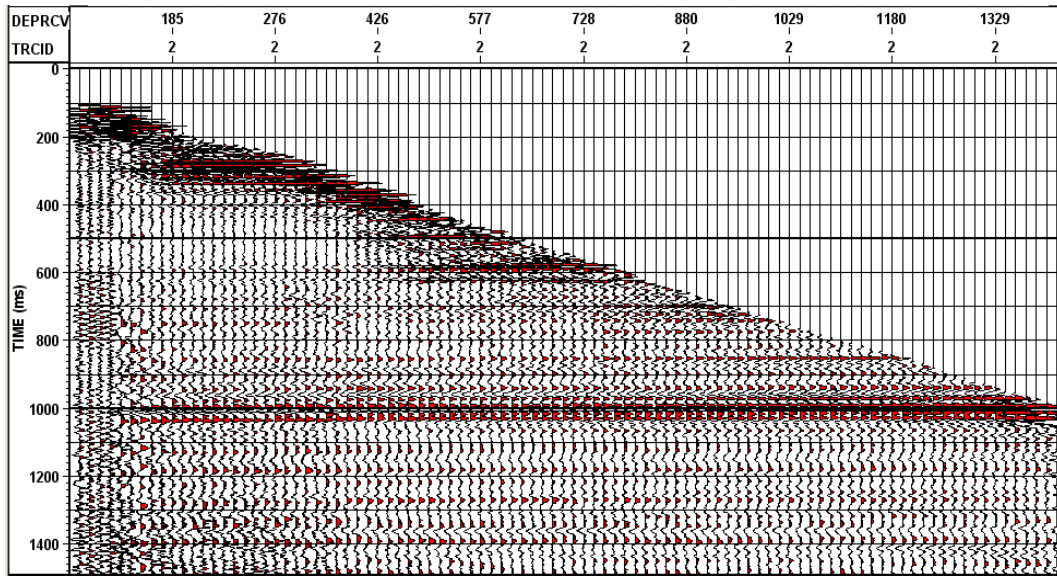
FIG. 19. Upgoing Z component in two-way-time Z(+TT) with AGC.

The vertical Z(FRT) undeconvolved data is now ready to be stacked. Figure 20 shows the stacking flow used to stack Z(FRT) and produce corridor stacks.
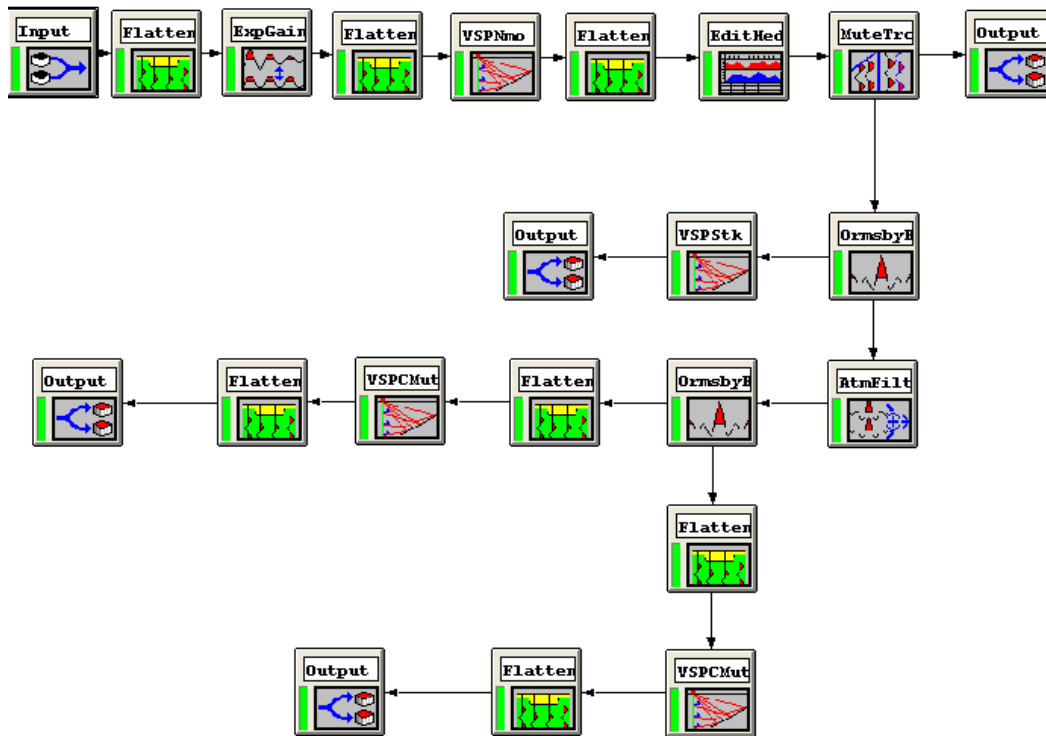


FIG. 20. Processing flow showing the process of stacking Z(FRT) into a full stack and corridor stacks.

The above flow deals with the undeconvolved upgoing median filtered Z(FRT) data. The data were flattened for the application of exponential gain of 1.5. Then the data was

converted back to Z(FRT) for the application of NMO correction, using the interval velocities calculated earlier from first breask, to ensure that events are in their proper times and will tie with surface seismic data in the future. The NMO-corrected data was then converted to two-way-time by multiplying the first breaks by two. A mute is applied to insure the correction of the VSP trace times for future true amplitude recovery. This produces the first output of Z(+TT) that is in two-way-time and NMO corrected. This result is then bandpass filtered to limit noise and replicated 10 times to produce a full stack. The Z(+TT) and NMO corrected data are median filtered with 4 point median filtering to enhance the signal to noise ratio. Furthermore the data is bandpass filtered and now two paths are created. The result is on situation converted back to Z(FRT), corridor muted and converted back to Z(+TT) to produce an inside corridor mute. The other situation is similar, only to produce outside corridor mute. A corridor mute of 80 ms and to a depth of 1220 m is applied to get the corridor muted data.  Figure 21 shows the flattened two-way-time Z(+TT) that is NMO corrected and Figure 22 is the same but with AGC. Figure 23 shows the undeconvolved full stack. Figures 24 and 25 show the outside and inside corridor mutes respectively.
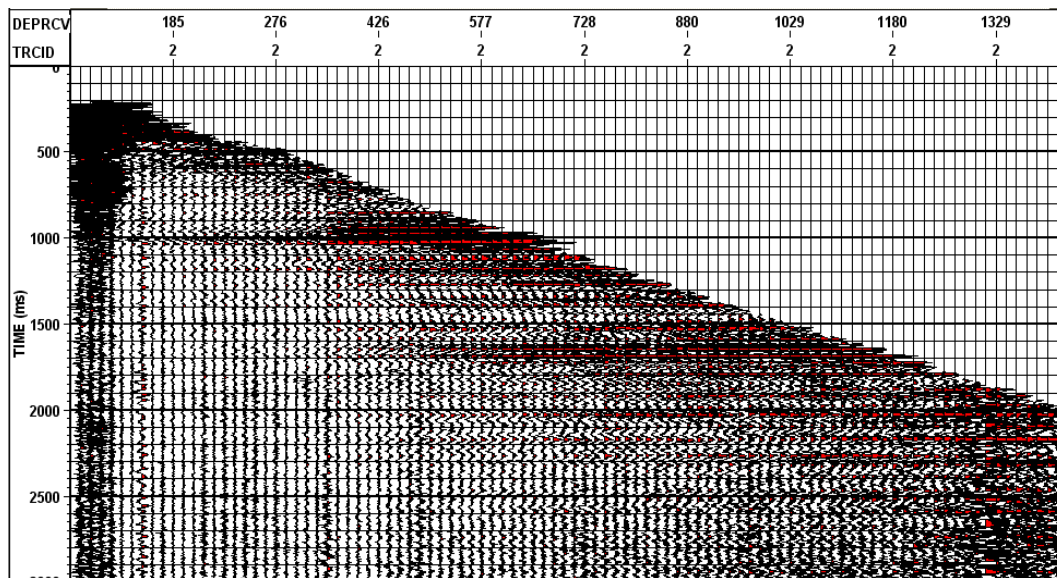


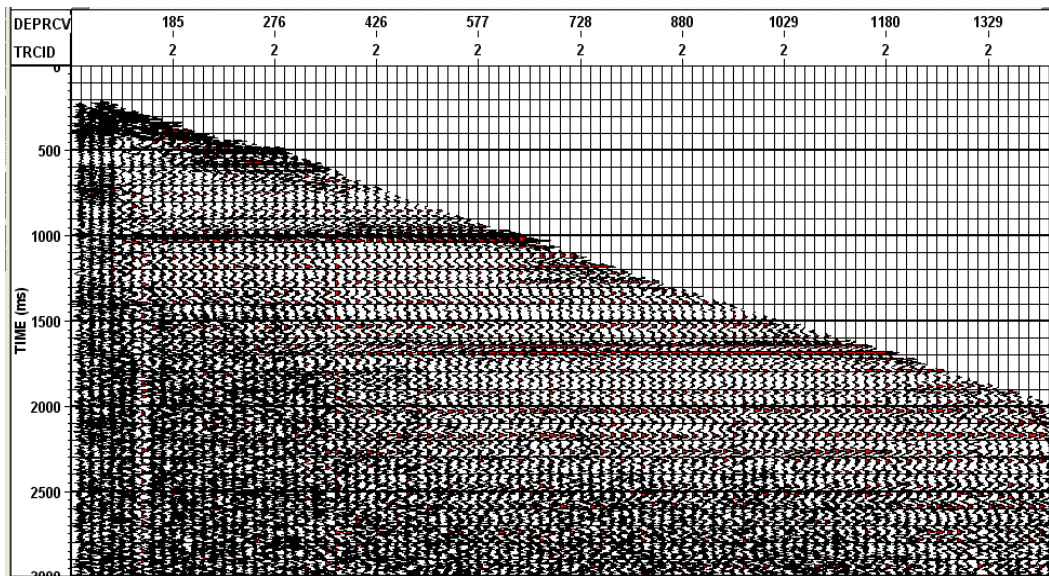FIG. 21. Flattened two-way-time Z(+TT) that is NMO corrected.

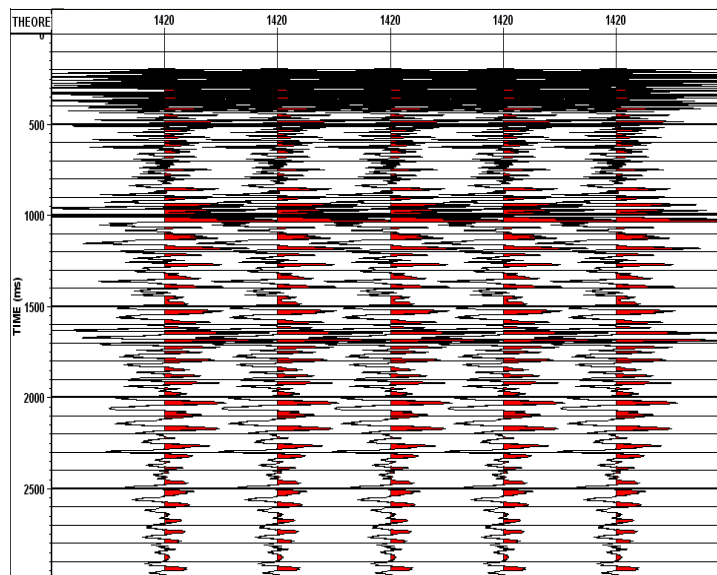FIG. 22. Flattened two-way-time Z(+TT) that is NMO corrected with AGC.



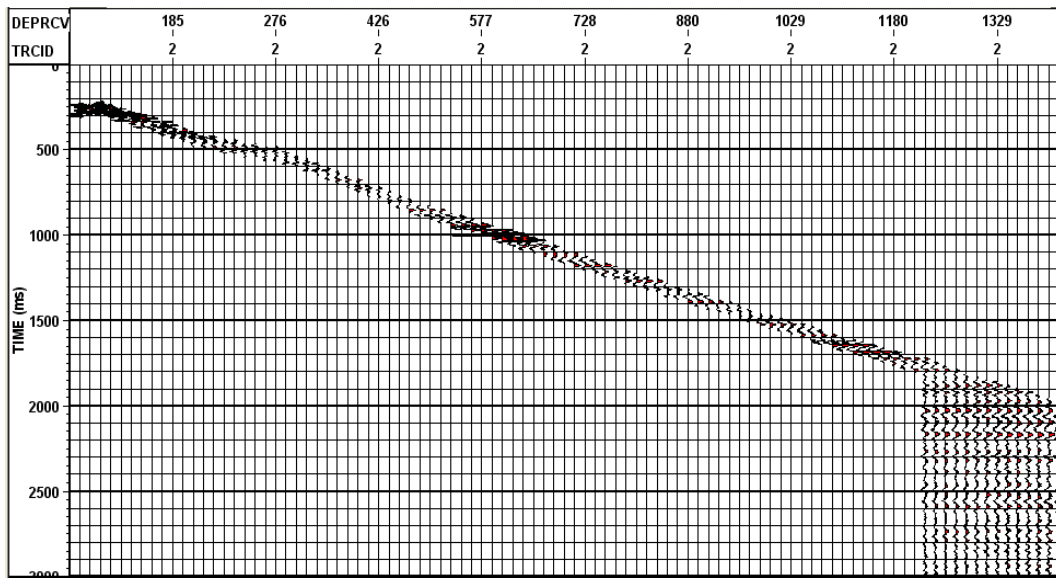FIG. 23. Z(+TT) Undeconvolved Full Stack.

FIG. 24. Z(+TT) undeconvolved outside corridor muted data with corridor length of 80 ms and muted to depth 1220 m.
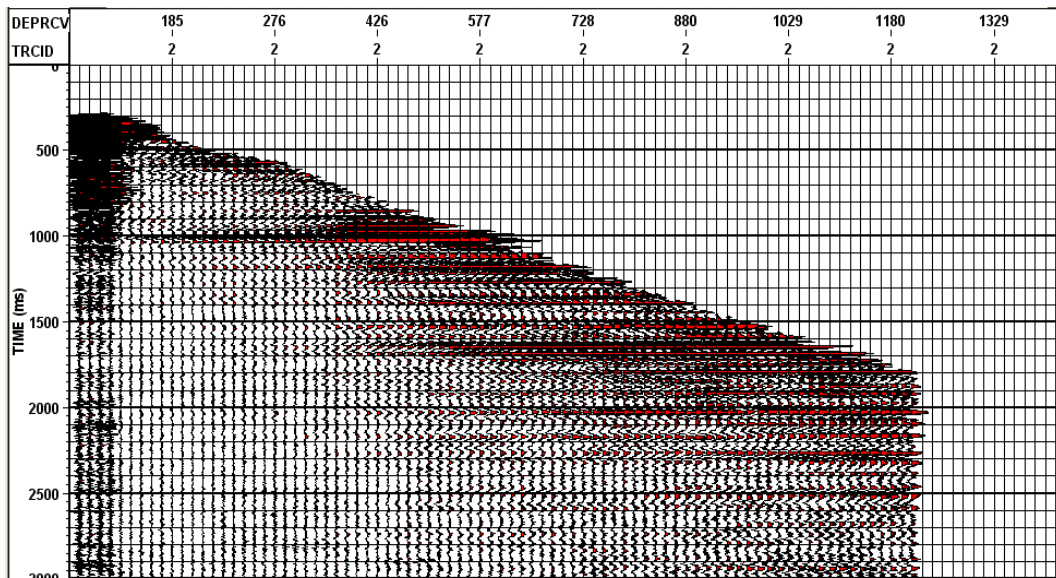


FIG. 25. Z(+TT) undeconvolved inside corridor muted data with corridor length of 80 ms and muted to depth 1220 m.

So far, the data that has been processed is still undeconvolved. The next logical step at this point is to deconvolve the data using the downgoing wavefield that represents the source signature and apply it to the upgoing waves. Figure 26 shows the deconvolution flow performed on Z(-TT) and applied to upgoing Z(-TT) to get upgoing deconvolved Z(FRT).
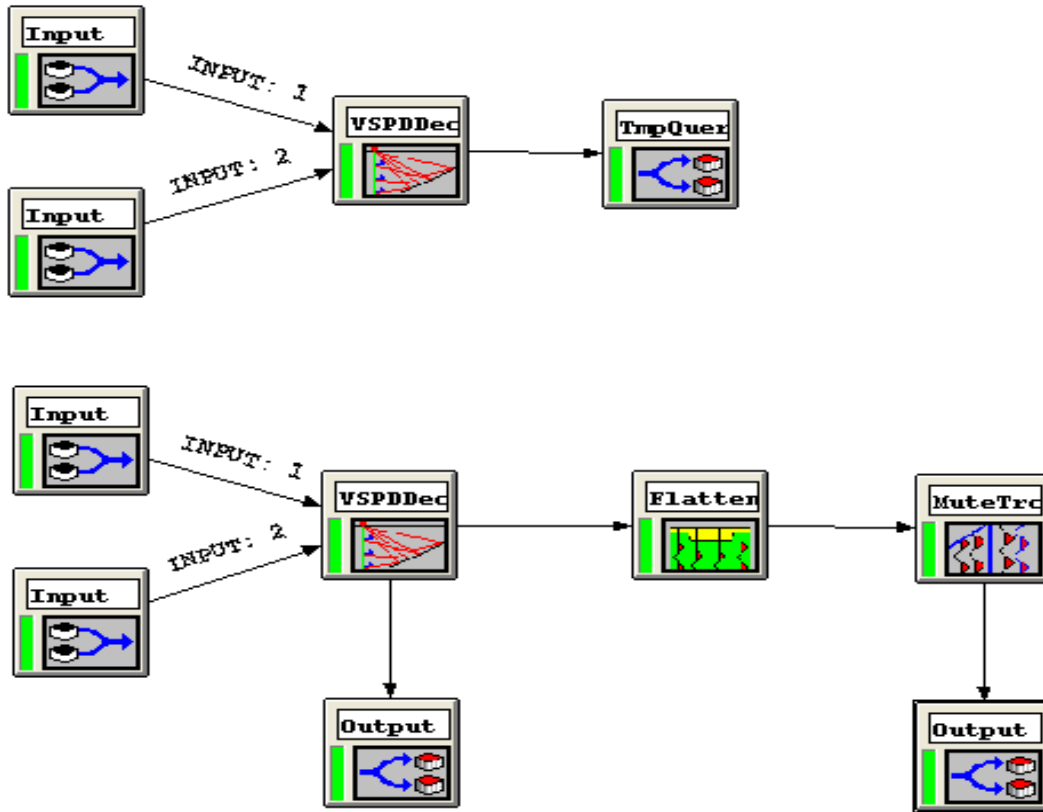
FIG. 26. Deconvolution flow performed on downgoing Z(-TT) and applied to upgoing Z(-TT) to get upgoing Z(FRT).

The upper part of the deconvolution flow shown in Figure 26 has downgoing Z(-TT) twice to optimize the deconvolution parameters. The deconvolution windows started at 0 ms and extended to 400 ms, 450 ms and 500 ms. After analysis of the result, I decided to go with the 400 ms window since it produced the best zero phased events that seem to be the most continuous. Figure 27 shows the resulting zero phased deconvolution operator. Figure 28 shows the deconvolved downgoing Z(-TT) as a result of the 400 ms window. Figure 29 shows the deconvolved upgoing Z(-TT) as a result of the 400 ms window. Also, Figure 30 shows the deconvolved upgoing Z(FRT) as a result of the 400 ms window.
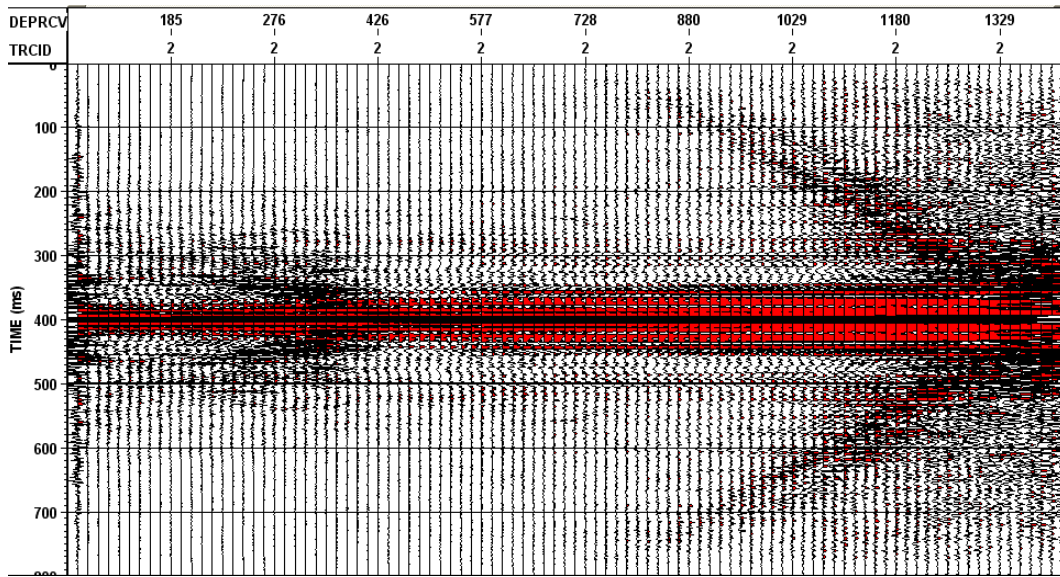
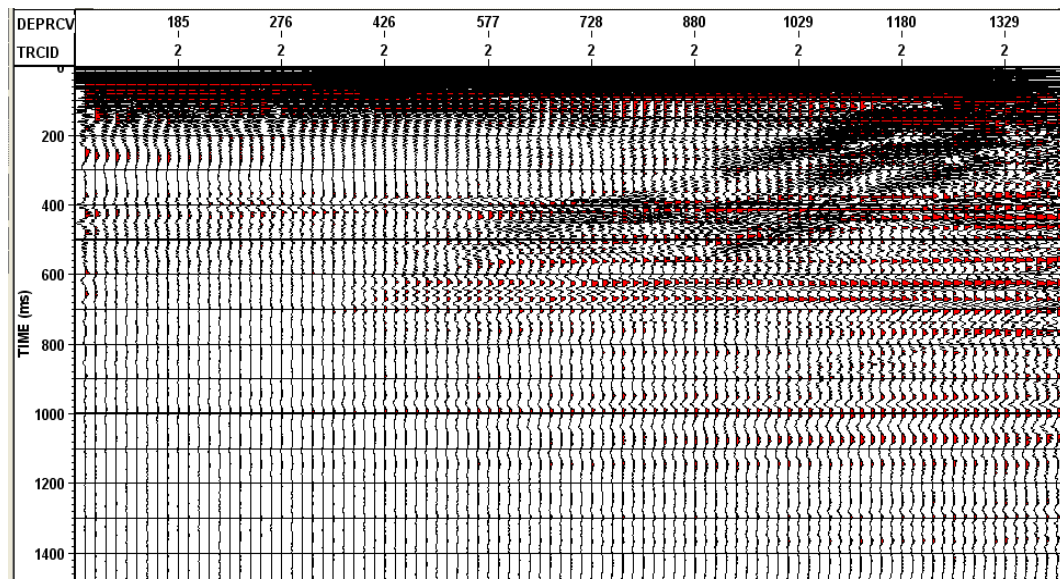FIG. 27. Deconvolution operator as a result of applying the 400 ms window.

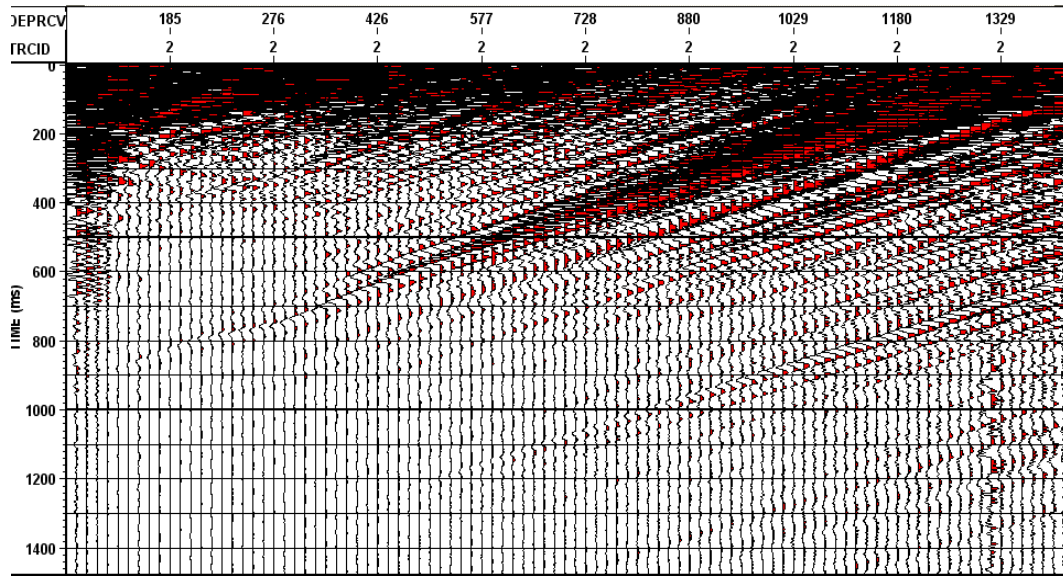FIG. 28. Deconvolved downgoing Z(-TT) as a result of the 400 ms window.

FIG. 29. Deconvolved upgoing Z(-TT) as a result of the 400 ms window.
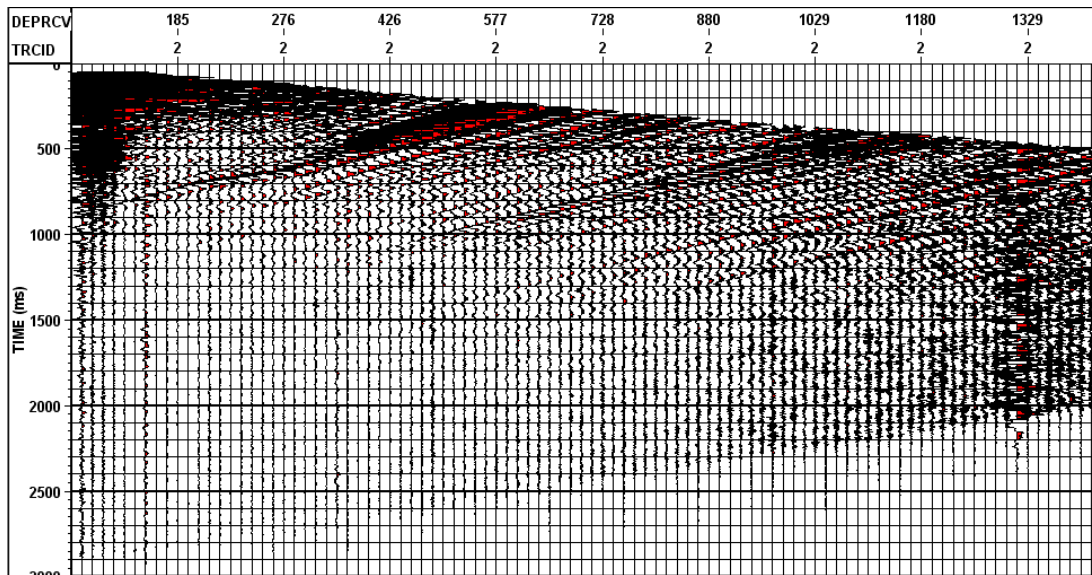


FIG. 30. Deconvolved upgoing Z(FRT) as a result of the 400 ms window.

Now that the data is deconvolved, now the need to develop full, inside and outside corridor mutes in pursued. The same flow displayed previously in Figure 20 is pursued again but this time the input data is the upgoing deconvolved median filtered NMO corrected Z(FRT). Figure 31 shows the flattened, deconvolved and NMO corrected two-way-time upgoing Z(+TT) while Figure 32 is the same but with AGC applied. Figure 33 shows the deconvolved full stack. Figure 34 shows the outside corridor mute and Figure 35 shows the inside corridor mute.
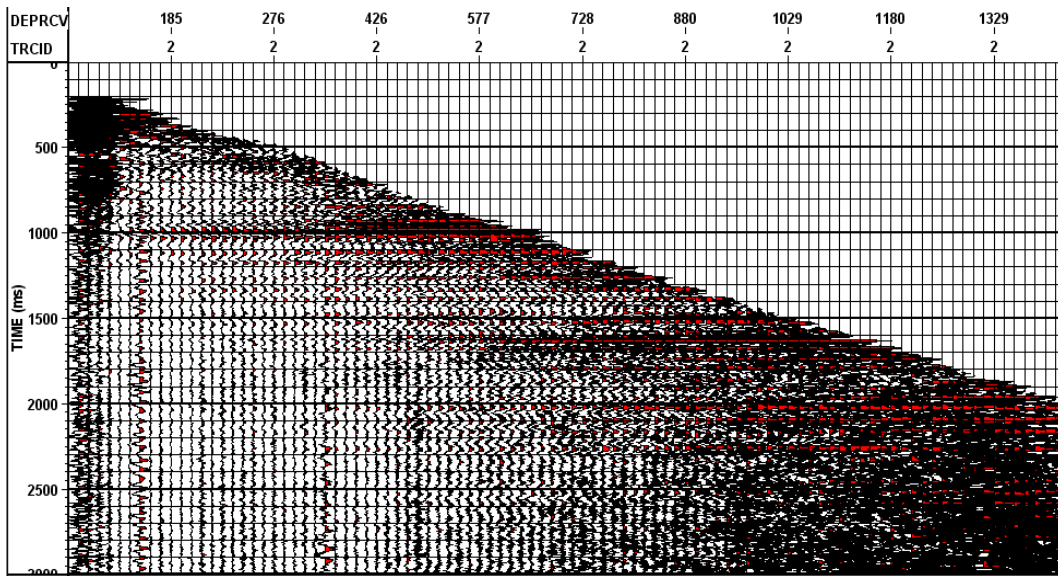
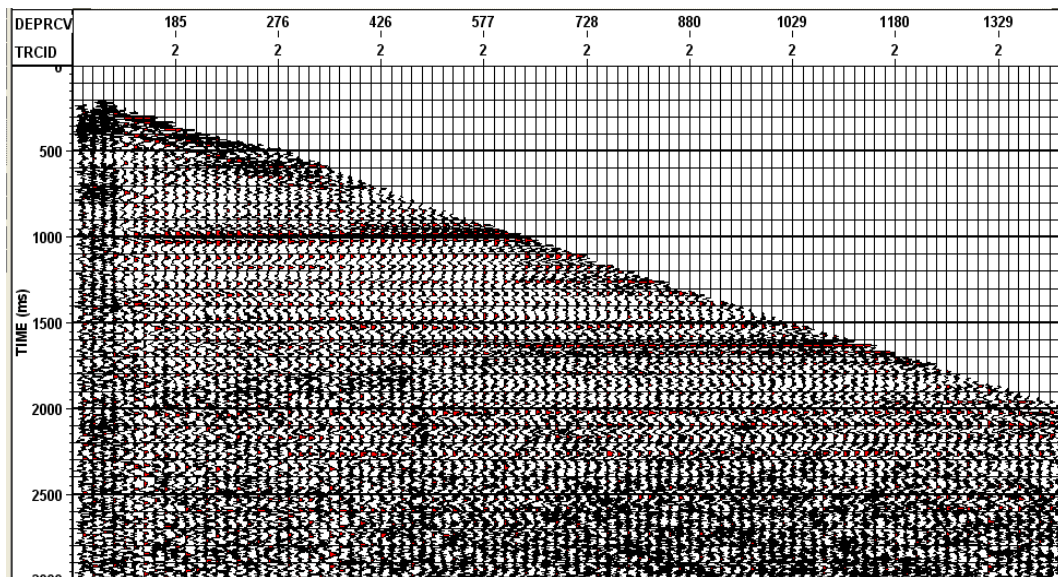FIG. 31. Flattened, deconvolved two-way-time Z(+TT) that is NMO corrected.



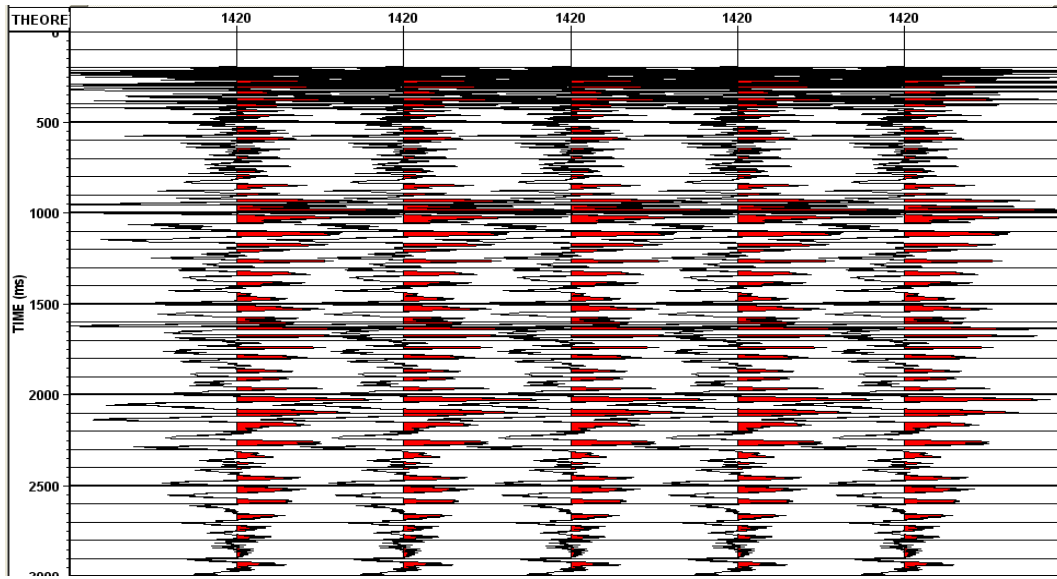FIG. 32. Flattened, deconvolved two-way-time Z(+TT) that is NMO corrected and with AGC.

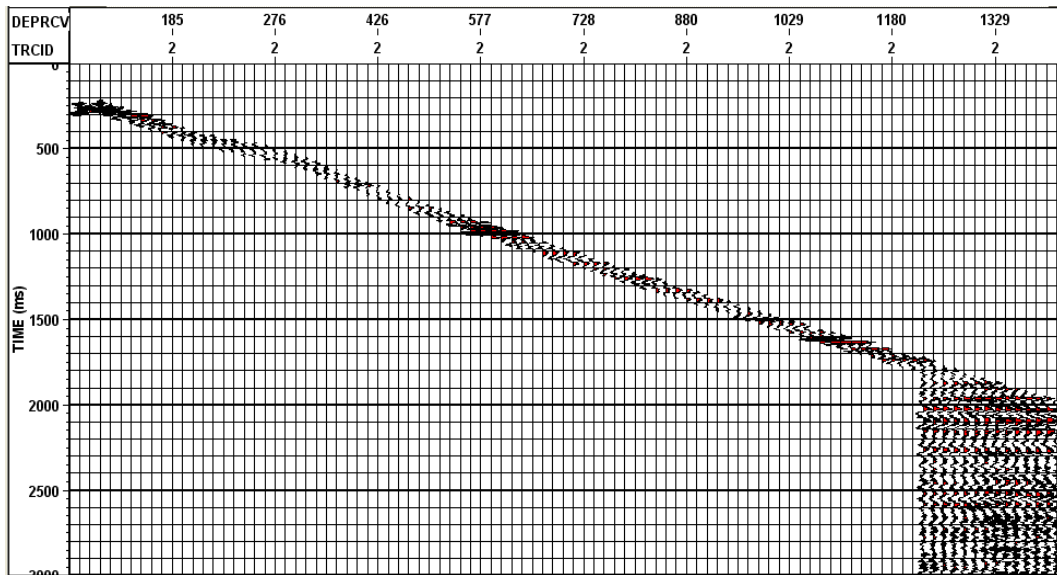FIG. 33. Deconvolved full stack.



FIG. 34. Z(+TT) deconvolved outside corridor muted data with corridor length of 80 ms and muted to depth 1220 m.
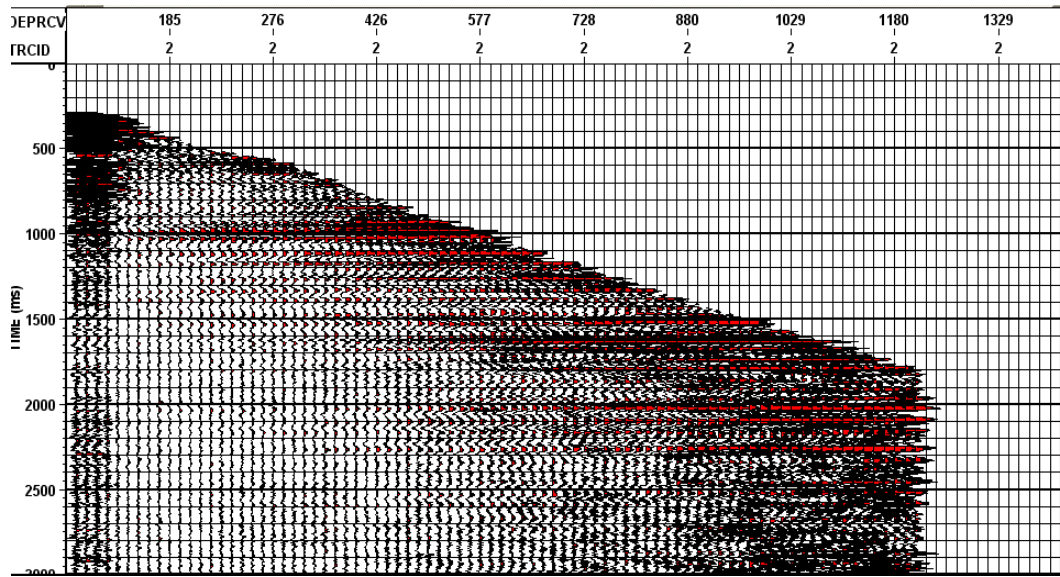
FIG. 35. Z(+TT) deconvolved inside corridor muted data with corridor length of 80 ms and muted to depth 1220 m.

Finally, both deconvolved inside and outside corridor stacks are displayed in Figures 36 and 37 respectively.
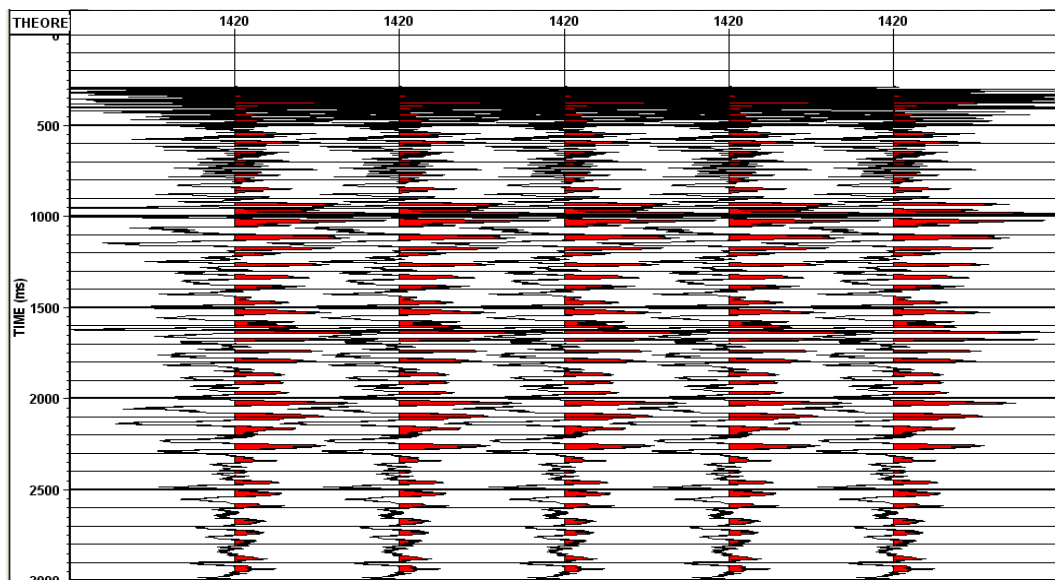


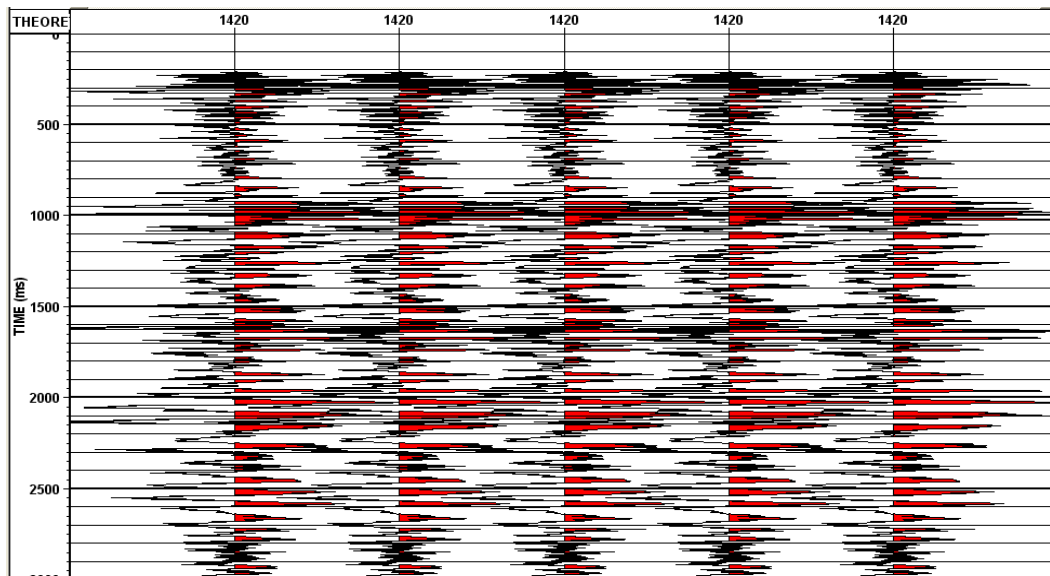FIG. 36. Stack after deconvolved inside corridor mute.

FIG. 37. Stack after deconvolved outside corridor mute.

## CONCLUSIONS

The zero-offset VSP was initially first break picked which enabled the calculation of interval velocities and was used to flatten the upgoing events. Next, wavefield separation was performed using 9, 11,13,14,15 point median filtering until the decision was made to use 13 point median filtering for further processing. The results were fully stacked and corridor stacked. Next, deconvolution windows were explored and varied between 400 ms and 500 ms. The decision was then made to go with the 400 ms window. Lastly, the deconvolved data was corridor and fully stacked.

Future work would include processing of the three azimuthal walkaway VSP surveys and further investigation and analysis of AVO for the Mannville coals and the overburden.

## AKNOWLEDGEMENTS

## REFERENCES

Bell., J.S., Bachu, S., 2003, In situ stress magnitude and orientation estimates for Cretaceous coal-bearing strata beneath the plains area of central and southern Alberta, Bulletin of Canadian Petroleum Geology, **51**, No. 1, pages 1-28.

Coulombe, C.A., 1993, Amplitude-Versus-Offset analysis using vertical seismic profiling and well log data, Master's Thesis, Department of Geology and Geophysics, The University of Calgary.

Hinds, R.C., Anderson, N.L., Kuzmiski, R.D., 1999, VSP Interpretive Processing: Theory and Practice, Society of Exploration Geophysicists.

Parker, R., Jones, M., 2008, Rig-source VSP/Sonic Calibration/Synthetics/Walkaway VSP Processing Report, Shlumberger, pages 5-14.

Stewart., R.R., 2001, VSP: An In Depth Seismic Understanding, Department of Geology and Geophysics, University of Calgary, CSEG Recorder, **26**, No. 7.